Dark solitons at nonlinear interfaces

Julio Sánchez-Curto,[1,*] **Pedro Chamorro-Posada,**[1] **and Graham S. McDonald**[2]
[1] *Departamento de Teoría de la Señal y Comunicaciones e Ingeniería Telemática, Universidad de Valladolid, ETSI Telecomunicación, Paseo Belén 15, Valladolid 47011, Spain*
[2] *Joule Physics Laboratory, School of Computing, Science and Engineering, University of Salford, Salford M5 4WT, United Kingdom and*
[*] *Corresponding author: julsan@tel.uva.es*

The refraction of dark solitons at a planar boundary separating two defocusing Kerr media is simulated and analyzed, for the first time. Analysis is based on the nonlinear Helmholtz equation, and is thus valid for any angle of incidence. A new law, governing refraction of black solitons, is combined with one describing bright soliton refraction, to yield a generalized Snell's law whose validity is verified numerically. The complexity of gray soliton refraction is also analyzed, and illustrated by a change from external to internal refraction on varying the soliton contrast parameter.

OCIS codes: 190.3270, 190.6135.

Solitons are universal nonlinear waves and material interfaces play a fundamental role as boundary conditions. In particular, spatial solitons are predicted to become key elements of emerging photonic technologies [1, 2]. The behaviour of soliton beams at nonlinear interfaces has been extensively treated in the literature, where Kerr-type, and also saturable-Kerr [3], photorefractive [4], and quadratic soliton [5, 6] refraction properties have been reviewed and proposed for the design of all-optical devices [7–10]. Most previous works on nonlinear interfaces have two features in common. First, analysis has been performed assuming the paraxial approximation, and using the nonlinear Schrödinger (NLS) equation as the soliton propagation model [11]. Second, previous studies only analyzed refraction properties of bright spatial solitons. In fact, only a few investigations have studied the behaviour of dark solitons at nonlinear interfaces in a paraxial context, where attention was restricted to nonlinear surface waves at Kerr-type media [12, 13] or to kink solitons arising at surfaces of optical lattices imprinted in defocusing media [14]. To the authors' knowledge, the refraction of dark solitons at nonlinear interfaces has not previously been studied.

Nonparaxial theory based on the nonlinear Helmholtz (NLH) equation [15, 16] permits one to overcome intrinsic angular limitations of NLS descriptions. In contrast to other nonparaxial regimes [17, 18], where effects have their origin in the strong focusing of high-intensity beams, we consider broad (compared to the optical wavelength) beams of moderate power. Nonparaxiality then arises solely from angular effects. Exact analytical solutions of NLH equations have been found in the form of bright Kerr [16], dark Kerr [19], two-component [20], and bistable [21] Helmholtz solitons, and have allowed extension of paraxial soliton theory to arbitrary-angle regimes. Soliton refraction effects have a strong inherent angular character and constitute an excellent testbed for nonparaxial Helmholtz theory [22, 23].

Spatial dark solitons present localized intensity dips on modulationally-stable plane waves [24]. In the physical realization of such nonlinear waves, the infinite background is replaced with a beam [25–27]. As with their bright counterparts, dark solitons have also been proposed for all-optical signal processing devices [27, 28].

In this Letter, the laws governing the refraction of Helmholtz dark solitons [19] at interfaces separating two defocusing Kerr media are presented. Figure 1(a) illustrates the geometry of soliton refraction, where a black soliton is incident at angle θ_i on an interface separating two defocusing Kerr media, and refracts at angle θ_t. The total refractive index of medium i is $n_{0i} - \alpha_i I$, where $\alpha_i > 0$ is the Kerr coefficient and I the optical intensity. Assuming a relatively low value of α_i, the approximation $n^2 \approx n_{0i}^2 - 2n_{0i}\alpha_i I$ is used.

For a TE optical field, the complex envelope u of a forward propagating beam evolves according to

$$\kappa\frac{\partial^2 u}{\partial\zeta^2} + j\frac{\partial u}{\partial\zeta} + \frac{1}{2}\frac{\partial^2 u}{\partial\xi^2} - |u|^2 u = \left[\frac{\Delta}{4\kappa} - (1-\alpha)|u|^2\right] H(\xi)u. \quad (1)$$

A derivation from the Helmholtz equation is detailed in [23]. Here, the focusing Kerr nonlinearity is replaced by a defocusing one. $H(\xi)$ is the Heaviside function, $\xi = 2^{1/2}x/w_0$ and $\zeta = z/L_D$ are the normalized transverse and longitudinal coordinates, respectively, and w_0 is the waist of a reference Gaussian beam with diffraction length $L_D = kw_0^2/2$. $\kappa = 1/k^2w_0^2$ is a nonparaxiality parameter, while $\Delta = 1 - n_{02}^2/n_{01}^2$ and $\alpha = \alpha_2/\alpha_1$ account for the linear and nonlinear refractive index mismatch at the interface, respectively.

The general Helmholtz dark soliton in the second

medium is [19]

$$u(\xi,\zeta) = u_0\left(A\tanh\Theta + jF\right)\exp\left(\frac{-j\zeta}{2\kappa}\right) \times \exp\left[j\sqrt{\frac{1-\Delta-4\kappa u_0^2\alpha}{1+2\kappa V^2}}\left(-V\xi+\frac{\zeta}{2\kappa}\right)\right] \quad (2)$$

where

$$\Theta = \frac{u_0 A\alpha^{1/2}\left(\xi+W\zeta\right)}{\sqrt{1+2\kappa W^2}} \quad \text{and} \quad \mathrm{W} = \frac{\mathrm{V}-\mathrm{V}_0}{1+2\kappa\mathrm{V}\mathrm{V}_0}. \quad (3)$$

V is a transverse velocity arising from an arbitrary rotation angle θ of the laboratory coordinates, $V = \tan(\theta)(2\kappa)^{-1/2}$ [15], and W is the net transverse velocity of the dark soliton resulting from the combination of V and the intrinsic transverse velocity

$$V_0 = u_0 F\alpha^{1/2}\left[1-\Delta-\left(2+F^2\right)2\kappa u_0^2\alpha\right]^{-1/2}. \quad (4)$$

$F = (1-A^2)^{1/2}$ is the soliton grayness/contrast parameter and u_0 is the background amplitude. The dark soliton solution in medium 1 [19] is recovered from Eqs. (2)-(4) by setting $\alpha = 1$ and $\Delta = 0$. Our study only addresses dark soliton refraction, since significant reflection of the supporting beam may destroy the plane background required for stable dark soliton propagation. Our analysis is, thus, necessarily restricted to cases with negligible beam reflection at the interface.

First, we consider black solitons. The law governing their refraction is derived from ensuring continuity of the phase of the supporting beam across the interface. Using Eq. (2), and $\tan^2(\theta) = 2\kappa V^2$, we find a generalized Snell's law for black and bright [22, 23] soliton refraction

$$\gamma_\pm n_{01}\cos(\theta_i) = n_{02}\cos(\theta_t) \quad (5)$$

where $\gamma_\pm = (1+4\kappa\beta_\pm)^{1/2}\left[1+4\kappa\beta_\pm\alpha(1-\Delta)^{-1}\right]^{-1/2}$ is a nonlinear correction term. The subscript identifies the result for bright (+) and black (−) Helmholtz solitons. In the case of bright solitons, one has [22, 23] $\beta_+ = \eta_0^2/2$ whereas for black solitons $\beta_- = -u_0^2$; the nonlinear role played by bright soliton amplitude (η_0) is thus replaced by the amplitude of the black soliton background. In physical terms, bright solitons are perfectly collimated nonlinear beams and behave at interfaces in a fashion similar to plane waves, but it is the nonlinear plane wave that determines the refraction of black solitons (which are linear at their core).

The value of γ_- is real, from an assumed condition of Helmholtz type of nonparaxiality: $4\kappa u_0^2 \ll 1$, which in turn implies that $\Delta + 4\kappa u_0^2\alpha < 1$. While the former condition establishes the physical restriction that the total refractive index in the first medium must remain positive [19], $2|\alpha_1|E_0^2 < n_{01}$, the latter determines an analogous restriction for the second medium, $2|\alpha_2|E_0^2 < n_{02}$.

The total (linear plus nonlinear) refractive index mismatch across the interface is given by $\delta_\pm = \Delta + 4\kappa\beta_\pm(1-\alpha)$. In the same way that δ_+ determines how bright solitons refract [23], δ_- can be used to interpret Snell's law for black soliton refraction at self-defocusing interfaces. In Fig. 1, three different cases of a black soliton impinging on an interface at 25° are studied. Figure 1(b) shows how a black soliton undergoes internal refraction for an interface with discontinuity only in the linear refractive index ($\Delta = 0.0024$ and $\delta_- > 0$). The case of an interface with exclusively nonlinear index mismatch, where one expects external refraction, is illustrated in Fig. 1(d) ($\alpha = 0.4$ and $\delta_- < 0$). With both mismatch contributions present, they may cancel when the transparency/nonrefracting condition ($\delta_- = 0$) is met. This is verified in Fig. 1(c), where the dip position does not deviate from the initial propagation direction.

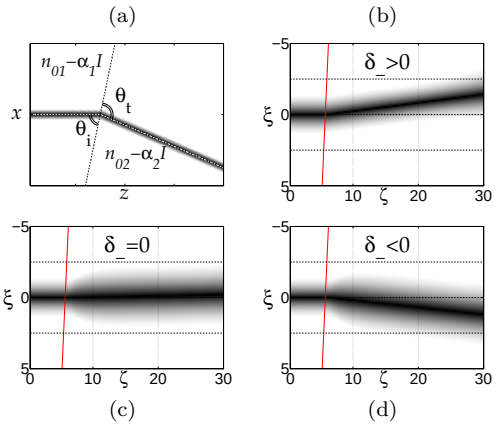

Fig. 1. (a) Refraction geometry. A black soliton experiencing: (b) internal refraction, (c) transparency, and (d) external refraction. Here, $u_0 = 1$ and $\kappa = 10^{-3}$, giving $\theta_t = 24.851°$, 25° and 25.147°, respectively. In scaled units, one obtains $W = 10.356$, 10.427 and 10.497.

The value of α not only affects the soliton angle of refraction but can also induce significant change in soliton width. The input field distribution for the second medium generally presents a perturbed-soliton initial condition [19, 29]. After crossing the interface, the soliton narrows ($\alpha > 1$) or broadens ($\alpha < 1$), and the emission of $2N_0$ gray solitons is expected, where N_0 is the largest integer satisfying $N_0 < \sqrt{\alpha}$ [19, 29].

Attention is now turned to the refraction of gray solitons. As for black ($F = 0$) solitons, the phase slope of the background beam associated with its transverse velocity V must be continuous across the interface. In the gray ($F \neq 0$) case, an additional independent condition arises from assuring the continuity of the phase structure of the supporting beam: the intrinsic phase jump of the gray soliton which, from Eq. (2), amounts to $-2\tan^{-1}(F/A)$ must be the same on both sides of the interface. It depends solely on the grayness parameter F, and its preservation upon refraction implies the conservation of F. Black (gray) solitons impinging the nonlinear interface are thus refracted as black (gray) solitons in the second medium.

Refraction properties of gray solitons are also dependent on the value of F. This effect is shown in Fig. 2, where two solitons with different values of F encounter the same interface ($\Delta = -0.016$ and $\alpha = 3$) with the same angle of incidence for the background beam $\theta_i = 30^o$. The left picture of Fig. 2 shows a gray soliton with $F = 0.05$ undergoing external refraction. However, internal refraction is experienced by the gray soliton with $F = 0.6$, as demonstrated in the right side of Fig. 2. Larger F entails a larger intrinsic velocity component, Eq. (4), and a smaller net transverse velocity, W. This reduces the angle of refraction until it is less than the angle of incidence. Refraction properties of gray solitons thus present novel features (not found in bright or black soliton refraction).

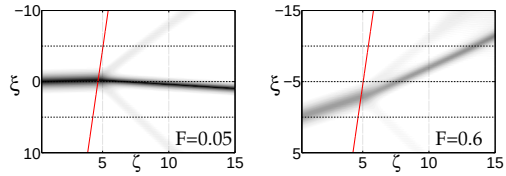

Fig. 2. External (left) and internal (right) refraction.

In this work, simulations have employed a nonparaxial beam propagation method [30] for the numerical integration of the NLH equation. Rotational symmetry [15] allowed us to consider solitons traveling with zero transverse velocity encountering an obliquely-orientated interface. The background beam, supporting the solitons, was a raised cosine $h(\xi) = \cos^2[\pi/rL(|\xi| - L_1)]$ if $L_1 < |\xi| < L_2$, $h(\xi) = 1$ if $|\xi| \leq L_1$ and $h(\xi) = 0$ if $|\xi| \geq L_2$, with roll-off factor $r = 0.5$, grid length $L = 160$, $L_1 = (1 - r)L/4$ and $L_2 = (1 + r)L/4$.

In summary, dark soliton refraction at interfaces separating two defocusing Kerr media has been analyzed for the first time. Analysis has been undertaken within the framework of Helmholtz theory, which yields valid results for beams propagating at arbitrary angles. We have provided a unified theory in which a compact generalised Snell's law describes the refraction of both bright and black solitons. Numerical results show excellent agreement with analytical predictions. Analysis of gray soliton refraction revealed a richer complexity that was explained in terms of the properties of the exact solutions. One key finding is that soliton grayness is conserved during refraction.

This work has been supported by the Spanish Ministerio de Educación y Ciencia and Fondo Europeo de Desarrollo Regional, project TEC2007-67429-C02-01, and Junta de Castilla y León, project VA001A08.

References

1. G.I. Stegeman and M. Segev, Science **286**, 1518 (1999).
2. S. Trillo and W. Torruellas, *Spatial solitons* (Springer Verlag, Berlin, 2000).
3. P.J. Bradley and C. De Angelis, Opt. Commun. **130**, 205 (1996).
4. A.D. Boardman, P. Bontemps, W. Ilecki, and A.A. Zharov, J. Mod. Opt. **47**, 1941 (2000).
5. I.V. Shadrivov and A.A. Zharov, J. Opt. Soc. Am. B **19**, 596 (2002).
6. I.V. Shadrivov and A.A. Zharov, Opt. Commun. **216**, 47 (2003).
7. D. Mihalache, M. Bertolotti, and C. Sibilia, Progr. Optics **27**, 227 (1989).
8. A.B. Aceves, J.V. Moloney, and A.C. Newell, Phys. Rev. A **39**, 1828 (1989).
9. J. Scheuer and M. Orenstein, J. Opt. Soc. Am. B **22**, 1260 (2005).
10. G. Cancellieri, F. Chiaraluce, E. Gambi, and P. Pierleoni, J. Opt. Soc. Am. B **12**, 1300 (1995).
11. A.B. Aceves, J.V. Moloney, and A.C. Newell, Phys. Rev. A **39**, 1809 (1989).
12. S.R. Skinner and D.R. Andersen, J. Opt. Soc. Am. B **8**, 759 (1991).
13. Y. Chen, Phys. Rev. A **45**, 4974 (1992).
14. Y.V. Kartashov, V.A. Vysloukh, and L. Torner, Opt. Express. **14**, 12365 (2006).
15. P. Chamorro-Posada, G.S. McDonald, and G.H.C. New, J. Mod. Opt. **45**, 1111 (1998).
16. P. Chamorro-Posada, G.S. McDonald, and G.H.C. New, J. Opt. Soc. Am. B **19**, 1216 (2002).
17. G. Fibich, Phys. Rev. Lett. **76**, 4356 (1996).
18. A. Ciattoni, B. Crosignani, S. Mookherjea, and A. Yariv, Opt. Lett. **30**, 516 (2005).
19. P. Chamorro-Posada and G.S. McDonald, Opt. Lett. **28**, 825 (2003).
20. J.M. Christian, G.S. McDonald, and P. Chamorro-Posada, Phys. Rev. E **74**, 066612 (2006).
21. J.M. Christian, G.S. McDonald, and P. Chamorro-Posada, Phys. Rev. A **76**, 033833 (2007).
22. J. Sánchez-Curto, P. Chamorro-Posada, and G.S. McDonald, Opt. Lett. **32**, 1126 (2007).
23. J. Sánchez-Curto, P. Chamorro-Posada, and G.S. McDonald, J. Opt. A: Pure Appl. Opt. **11**, 054015 (2009).
24. Yu.S. Kivshar and B. Luther-Davies, Phys. Rep. **298**, 81 (1998).
25. D.R. Andersen, D.E. Hooton, G.A. Swartzlander, Jr., and A.E. Kaplan, Opt. Lett. **15**, 783 (1990).
26. G.A. Swartzlander, Jr., D.R. Andersen, J.J. Regan, H. Yin, and A.E. Kaplan, Phys. Rev. Lett. **66**, 1583 (1991).
27. M.D. Iturbe-Castillo, J.J. Sánchez-Mondragón, S.I. Stepanov, M.B. Klein, and B.A. Wechsler, Opt. Commun. **118**, 515 (1995).
28. B. Luther-Davies and Y. Xiaoping, Opt. Lett. **17**, 496 (1992).
29. Yu.S. Kivshar, IEEE J. Quantum Electron. **29**, 250 (1993).
30. P. Chamorro-Posada, G.S. McDonald, and G.H.C. New, Opt. Commun. **192**, 1 (2001).